A square-well model for the structural and thermodynamic properties of simple colloidal systems

L. Acedo
Departamento de Física, Universidad de Extremadura, E-06071 Badajoz, Spain

A. Santos[a)]
Department of Physics, University of Florida, Gainesville, Florida 32611

A model for the radial distribution function $g(r)$ of a square-well fluid of variable width previously proposed [Yuste and Santos, J. Chem. Phys. **101**, 2355 (1994)] is revisited and simplified. The model provides an explicit expression for the Laplace transform of $rg(r)$, the coefficients being given as explicit functions of the density, the temperature, and the interaction range. In the limits corresponding to hard spheres and sticky hard spheres, the model reduces to the analytical solutions of the Percus–Yevick equation for those potentials. The results can be useful to describe in a fully analytical way the structural and thermodynamic behavior of colloidal suspensions modeled as hard-core particles with a short-range attraction. Comparison with computer simulation data shows a general good agreement, even for relatively wide wells. © *2001 American Institute of Physics.* [DOI: 10.1063/1.1384419]

I. INTRODUCTION

In the simplest model of a colloidal dispersion, the interactions among the (large) solute molecules and the excluded volume effects of the (small) solvent molecules, which lead to intercolloidal solvation forces, are incorporated by treating the solute particles as hard spheres (HS) of diameter σ. This allows one to take advantage of the analytical solution of the Percus–Yevick (PY) integral equation for the HS potential.[1,2] On the other hand, it is well known that the solvent particles (e.g., macromolecules) can induce an effective short-range attraction between two colloidal particles due to an unbalanced osmotic pressure arising from depletion of the solvent particles in the region between the two colloidal ones.[3–6] This explains the widespread use of Baxter's model of sticky hard spheres (SHS)[7] to represent the properties of colloidal suspensions.[8–19] This interaction model represents the attractive part of the potential as an infinitely deep, infinitely narrow well. In addition to the hard-core diameter σ, the model incorporates a "stickiness" parameter τ_{SHS}^{-1} (essentially the deviation of the second virial coefficient from the HS value) that can be understood as a measure of the temperature: the smaller the temperature, the larger the stickiness. The SHS potential has the advantage of lending itself to an analytical solution in the PY approximation[7] and in the mean spherical approximation (MSA).[20] On the other hand, the SHS potential presents two limitations. First, the system of monodisperse SHS is not thermodynamically stable;[21,22] however, this pathology, which is not captured by Baxter's solution to the PY equation, can be remedied by including some degree of polydispersity in the system. The most important limitation of the SHS model as a representation of a realistic short-range interaction lies in the fact that it is unable to distinguish two situations with the same "stickiness" (i.e., same second virial coefficient) and density, but different temperature and/or range.

In order to mimic the particle interaction in colloidal systems in a more realistic way, a simple choice is to assume that the particles interact via the square-well (SW) potential[23–25]

$$\varphi(r) = \begin{cases} \infty, & r < \sigma \\ -\epsilon, & \sigma < r < \lambda\sigma \\ 0, & r > \lambda\sigma, \end{cases} \tag{1.1}$$

where σ is the diameter of the hard core, ϵ is the well depth, and $(\lambda - 1)\sigma$ is the well width. The equilibrium properties of a SW fluid depend on the values of three dimensionless parameters: the reduced number density $\rho^* = \rho\sigma^3$, the reduced temperature $T^* = k_B T/\epsilon$ (k_B being the Boltzmann constant), and the width parameter λ. In the limits $\epsilon \to 0$ (i.e., $T^* \to \infty$) and/or $\lambda \to 1$, the SW fluid becomes the HS fluid. In addition, the SHS fluid[7] is obtained by taking the limits $\epsilon \to \infty$ (i.e., $T^* \to 0$) and $\lambda \to 1$, while keeping the stickiness parameter $\tau_{\text{SHS}}^{-1} = 12(\lambda - 1)(e^{1/T^*} - 1)$ constant. If we define in the original SW fluid a generalized stickiness parameter $\tau_{\text{SW}}^{-1} = 4(\lambda^3 - 1)(e^{1/T^*} - 1)$ as being proportional to the deviation of the second virial coefficient from the HS value,[26] then at a given density ρ^* the parameter space can be taken as the plane $(\tau_{\text{SW}}^{-1}, \lambda)$. The SHS limit explores the line $(\tau_{\text{SW}}^{-1}, \lambda = 1)$ only, while the HS model corresponds to the point $(\tau_{\text{SW}}^{-1}, \lambda) = (0, 1)$. This geometrical picture illustrates why the SW interaction model can be useful to uncover a much richer spectrum of values for the relevant parameters of the problem, even if the attraction range is relatively short.

Despite the mathematical simplicity of the SW potential, no analytical solution of the conventional integral equations for fluids (Yvon-Born-Green, hypernetted-chain, PY, . . .) is

---
[a)]Permanent address: Departamento de Física, Universidad de Extremadura, E-06071 Badajoz, Spain. Electronic mail: andres@unex.es

known.[27,28] The mean spherical model approximation of Sharma and Sharma[29] provides an analytical expression for the structure factor, but it is not consistent with the hard-core exclusion constraint. Most of the available theoretical information about the SW fluid for variable width comes from perturbation theory.[30–38] In general, perturbation theory is based on an expansion of the relevant physical quantities in powers of the inverse temperature. For instance, the radial distribution function $g(r;\rho^*,T^*)$ of the SW fluid is expressed as

$$g(r;\rho^*,T^*) = g_0(r;\rho^*) + T^{*-1}g_1(r;\rho^*) + \cdots, \quad (1.2)$$

where $g_0(r;\rho^*)$ is the radial distribution function of the reference HS fluid and $g_1(r;\rho^*)$ represents a first-order correction. Good analytical approximations for g_0 are known, such as Wertheim–Thiele's solution of the PY equation,[1,2] Verlet–Weiss parameterization,[27] or the generalized mean spherical approximation.[39,40] Thus, it is in the choice of g_1 where different versions of perturbation theory essentially differ. A few years ago, Tang and Lu (TL)[36,37] proposed an analytical expression (in Laplace space) for g_1, based on the MSA. Comparison with Monte Carlo (MC) simulation data[41] showed a general good agreement for the cases considered, but the quality of the agreement worsened as smaller values of λ and/or T^* were taken. The expectation that perturbation theory becomes less accurate as the well width and the temperature decrease has already been reported elsewhere.[33,34] In fact, perturbation theory tends to overestimate the critical temperature T_c^*, especially for small values of $\lambda - 1$.[33,34] All these limitations are significantly apparent in the SHS limit ($\lambda \to 1$, $T^* \to 0$), in which case the expansion (1.2) becomes meaningless. By following a completely different approach, Nezbeda[42] proposed to approximate $rg(r)$ in the interval $\sigma \leq r \leq \lambda\sigma$ by a quadratic function of r, within the context of the PY theory. The coefficients of the polynomial were then determined analytically by imposing the continuity of the cavity function $y(r) \equiv g(r)e^{\varphi(r)/k_BT}$ and its first two derivatives at $r = \sigma$. Notwithstanding the merits of this theory, its main limitation is that it is only applicable for very narrow wells, typically $\lambda - 1 \lesssim 0.01$.[23,42,43] In addition, Nezbeda's theory fails to predict a thermodynamic critical point, except at $\lambda = 1$, in which case Baxter's solution for SHS is recovered.[42]

In order to provide a simple theory that, while including the SHS case as a special limit, could also be applicable to SW fluids of variable width, Yuste and Santos proposed a model by assuming an explicit functional form for the Laplace transform $G(t)$ of $rg(r)$.[44] That functional form was suggested by the exact virial expansion of the radial distribution function[45] and by the property $\lim_{r \to \sigma^+} g(r)$ = finite. The parameters were subsequently determined as functions of ρ^*, T^*, and λ by imposing the condition $S(0)$ = finite, where $S(q)$ is the structure function, as well as the continuity of $y(r)$ at $r = \lambda\sigma$. The structural properties predicted by the model showed a good agreement with MC simulation results, not only for narrow square wells, but even for relatively wide ones ($\lambda \approx 1.5$) up to densities slightly above the critical density.[44] On the other hand, the model was not fully analytical because the continuity condition of

$y(r)$ at $r = \lambda\sigma$ gives rise to a transcendent equation that must be solved numerically. In fact, the *exact* solution in the case of one-dimensional SW fluids involves a similar transcendent equation.[44,46]

The aim of this paper is to propose a simpler version of the model introduced by Yuste and Santos in Ref. 44. While we keep the same functional structure of $G(t)$ and enforce the conditions $g(\sigma^+)$ = finite and $S(0)$ = finite, we replace the transcendent equation stemming from the continuity of $y(r)$ at $r = \lambda\sigma$ by a quadratic equation suggested by the SHS limit. The resulting model therefore has a degree of algebraic simplicity similar to that of the PY solution for SHS (but now the parameters have a λ dependence beyond the one captured by the stickiness coefficient) and reduces to it in the appropriate limit. The structural properties $g(r)$ and $S(q)$ exhibit a fairly good agreement with MC simulations,[33,47] similar to that found in the original, more complicated version of the model.[44] Nevertheless, it is in the calculation of the thermodynamic properties (which were not addressed in Ref. 44) where the present model becomes especially advantageous. In particular, the isothermal compressibility is obtained as an explicit function of density, temperature, and well width. This allows us to get the λ dependence of the critical temperature T_c^* and density ρ_c^*. Comparison with computer simulation estimates[48] shows that the model predictions for $T_c^*(\lambda)$ are remarkably good, even for values of λ as large as $\lambda = 1.75$. On the other hand, the predicted values of $\rho_c^*(\lambda)$ are typically 30%–45% smaller than the simulation ones, a fact that can be traced back to the solution of the PY equation for SHS. We also compare the predictions of the model for the compressibility factor at $\lambda = 1.125$ and $\lambda = 1.4$ with simulation data[33,49] and with the TL perturbation theory.[37] In both cases the model presents a better agreement than the perturbation theory, except for temperatures larger than about twice the critical temperature.

The paper is organized as follows. The model is introduced and worked out in Sec. II, with some technicalities being relegated to the appendices. Section III deals with the comparison with simulation results and perturbation theory. The paper ends with a brief discussion in Sec. IV.

II. THE MODEL

A. Basic requirements

The radial distribution function $g(r)$ of a fluid is directly related to the probability of finding two particles separated by a distance r.[50] It can be measured from neutron- or x-ray diffraction experiments through the static structure factor $S(q)$. Both quantities are related by Fourier transforms

$$S(q) = 1 + \rho \int d\mathbf{r}\, e^{-i\mathbf{q}\cdot\mathbf{r}}[g(r) - 1]$$

$$= 1 - 2\pi\rho \left. \frac{G(t) - G(-t)}{t} \right|_{t=iq}, \quad (2.1)$$

where ρ is the number density and

$$G(t) = \int_0^\infty dr\, e^{-rt}rg(r) \quad (2.2)$$

J. Chem. Phys., Vol. 115, No. 6, 8 August 2001

Square-well model for colloidal systems   2807

is the Laplace transform of $rg(r)$. The isothermal compressibility of the fluid, $\kappa_T = \rho^{-1}(\partial\rho/\partial p)_T$, is directly related to the long-wavelength limit of the structure function,

$$\chi_T \equiv \rho k_B T \kappa_T = S(0). \tag{2.3}$$

Thus, all the physically relevant information about the equilibrium state of the system is contained in $g(r)$ or, equivalently, in $G(t)$.

Now, we particularize to the SW interaction potential, Eq. (1.1), so $g(r) = 0$ for $r < \sigma$. Henceforth, we will take the hard-core diameter $\sigma = 1$ as the length unit and the well depth $\epsilon/k_B = 1$ as the temperature unit, so that the asterisks in ρ^* and T^* will be dropped. It is convenient to define an auxiliary function $F(t)$ through the relation

$$G(t) = t\frac{F(t)e^{-t}}{1 + 12\eta F(t)e^{-t}}$$

$$= \sum_{n=1}^{\infty} (-12\eta)^{n-1}t[F(t)]^n e^{-nt}, \tag{2.4}$$

where $\eta \equiv (\pi/6)\rho\sigma^3$ is the packing fraction. Laplace inversion of Eq. (2.4) provides an useful representation of the radial distribution function

$$g(r) = r^{-1}\sum_{n=1}^{\infty} (-12\eta)^{n-1}f_n(r-n)\Theta(r-n), \tag{2.5}$$

where $f_n(r)$ is the inverse Laplace transform of $t[F(t)]^n$ and $\Theta(r)$ is Heaviside's step function. Thus, the knowledge of $F(t)$ is fully equivalent to that of $g(r)$ or $S(q)$. In particular, the value of $g(r)$ at contact, $g(1^+)$, is given by the asymptotic behavior of $F(t)$ for large t

$$g(1^+) = f_1(0) = \lim_{t \to \infty} t^2 F(t). \tag{2.6}$$

Since $g(1^+)$ must be finite and different from zero, we get the condition

$$F(t) \sim t^{-2}, \quad t \to \infty. \tag{2.7}$$

On the other hand, according to Eq. (2.1), the behavior of $G(t)$ for small t determines the value of $S(0)$

$$G(t) = t^{-2} + \text{const} + \frac{1 - S(0)}{24\eta}t + o(t^2). \tag{2.8}$$

Insertion of Eq. (2.8) into the first equality of Eq. (2.4) yields the first five terms in the expansion of $F(t)$ in powers of t,[39,40]

$$F(t) = -\frac{1}{12\eta}\left(1 + t + \frac{1}{2}t^2 + \frac{1+2\eta}{12\eta}t^3 + \frac{2+\eta}{24\eta}t^4\right)$$

$$+ \mathcal{O}(t^5). \tag{2.9}$$

The value of $S(0)$ is related to the coefficients of t^5 and t^6 by

$$S(0) = \frac{24}{5}\eta^3\left[6\frac{d^5F(t)}{dt^5}\bigg|_{t=0} - \frac{d^6F(t)}{dt^6}\bigg|_{t=0}\right]$$

$$-1 + 8\eta + 2\eta^2. \tag{2.10}$$

So far, all the expressions apply to any density and any hard-core potential. As is well known, in the limit of zero density the cavity function $y(r) \equiv g(r)e^{\varphi(r)/k_B T}$ is equal to 1.[50] In the special case of the SW potential, this translates into

$$\lim_{\eta \to 0} g(r) = (1+x)\Theta(r-1) - x\Theta(r-\lambda), \tag{2.11}$$

where $x \equiv e^{1/T} - 1$. Equation (2.11) implies that

$$\lim_{\eta \to 0} F(t) = (1+x)(t^{-2} + t^{-3}) - xe^{-(\lambda-1)t}(\lambda t^{-2} + t^{-3}). \tag{2.12}$$

B. Construction of the model

Any meaningful approximation of $F(t)$ for the SW potential must comply with Eqs. (2.7), (2.9), and (2.12). Let us decompose $F(t)$ as

$$F(t) = R(t) - \bar{R}(t)e^{-(\lambda-1)t}. \tag{2.13}$$

The model proposed by Yuste and Santos[44] consists of assuming the following rational forms for $R(t)$ and $\bar{R}(t)$:

$$R(t) = \frac{A_0 + A_1 t}{1 + S_1 t + S_2 t^2 + S_3 t^3}, \tag{2.14}$$

$$\bar{R}(t) = \frac{\bar{A}_0 + \bar{A}_1 t}{1 + S_1 t + S_2 t^2 + S_3 t^3}.$$

These forms are compatible with (2.12). In addition, condition (2.7) is satisfied by construction. In fact, the contact value is, according to Eq. (2.6)

$$g(1^+) = \frac{A_1}{S_3}. \tag{2.15}$$

In order to ease the proof that the HS and SHS cases are included in Eq. (2.14), it is convenient to introduce the new parameters $A \equiv -12\eta\bar{A}_0$, $L_1 \equiv -12\eta[\bar{A}_0(\lambda-1) + A_1 - \bar{A}_1]$, and $L_2 \equiv -12\eta\bar{A}_1(\lambda-1)$. With these changes, Eqs. (2.13) and (2.14) can be recast into

$$F(t) = -\frac{1}{12\eta}\frac{1+A+[L_1+L_2(\lambda-1)^{-1}-A(\lambda-1)]t-[A+L_2(\lambda-1)^{-1}t]e^{-(\lambda-1)t}}{1+S_1t+S_2t^2+S_3t^3}, \tag{2.16}$$

where we have already taken into account the property $F(0)=-1/12\eta$, according to Eq. (2.9). The model (2.16) contains six parameters to be determined. The exact expansion (2.9) imposes four constraints among them. Thus, we can express four of the parameters in terms of, for instance, A and L_2. The result is

$$L_1=\frac{1}{1+2\eta}\left[1+\frac{1}{2}\eta+2\eta(1+\lambda+\lambda^2)L_2\right.$$
$$\left.-\frac{1}{2}\eta(3+2\lambda+\lambda^2)A'\right], \tag{2.17}$$

$$S_1=\frac{\eta}{1+2\eta}\left[-\frac{3}{2}+2(1+\lambda+\lambda^2)L_2\right.$$
$$\left.-\frac{1}{2}(3+2\lambda+\lambda^2)A'\right], \tag{2.18}$$

$$S_2=\frac{1}{2(1+2\eta)}\{-1+\eta+2[1-2\eta\lambda(1+\lambda)]L_2$$
$$-[1-\eta(1+\lambda)^2]A'\}, \tag{2.19}$$

$$S_3=\frac{1}{1+2\eta}\left\{-\frac{(1-\eta)^2}{12\eta}-\left[\frac{1}{2}(\lambda+1)-\eta\lambda^2\right]L_2\right.$$
$$\left.+\frac{1}{12}[4+2\lambda-\eta(3\lambda^2+2\lambda+1)]A'\right\}, \tag{2.20}$$

where $A'\equiv A(\lambda-1)^2$. These four parameters are linear functions of A and L_2. Taking into account Eq. (2.10), the value of $S(0)$ can be expressed as a quadratic function of A and L_2. Its explicit expression is given in Appendix A.

Two additional constraints are still needed to determine A and L_2. First, note that in the zero-density limit we have $L_1\rightarrow1$, $S_1\rightarrow0$, $S_2\rightarrow$finite, $S_3\rightarrow-(12\eta)^{-1}$. Thus, Eq. (2.16) is consistent with Eq. (2.12) provided that

$$\lim_{\eta\rightarrow0}A=x, \quad \lim_{\eta\rightarrow0}L_2=x\lambda(\lambda-1). \tag{2.21}$$

In the original formulation of the model,[44] the parameter A was assumed to be independent of density, so that $A=x$. As for L_2, it was determined by imposing the (exact) continuity condition of the function $y(r)$ at $r=\lambda$,[27,51] which implies

$$g(\lambda^-)=(1+x)g(\lambda^+). \tag{2.22}$$

The implementation of this condition in the model (2.16) leads to a transcendent equation that must be solved numerically.[44] In this paper we will be concerned with a simpler version of the model in which the strong condition (2.22) is replaced by a weaker one. To that end, let us introduce a parameter τ as

$$\tau\equiv\frac{1}{12}\left(\frac{L_1}{L_2}-\frac{S_2}{S_3}\right). \tag{2.23}$$

From (2.21) and (2.23) it follows that

$$\lim_{\eta\rightarrow0}\tau=[12x\lambda(\lambda-1)]^{-1}. \tag{2.24}$$

The definition (2.23) is suggested by the fact that, as proved in Appendix B of Ref. 44, Eq. (2.22) is equivalent to $\tau=\tau_{SHS}$ in the SHS limit, namely $x\rightarrow\infty$, $\lambda\rightarrow1$, $x(\lambda-1)\equiv(12\tau_{SHS})^{-1}=$finite. Therefore, we may expect that a simple prescription for τ [such that $\tau^{-1}\rightarrow12x(\lambda-1)$ in the SHS limit] can be a good substitute for the transcendent equation arising from (2.22), at least for relatively narrow wells.

Since L_1, S_2, and S_3 are linear functions of L_2. Eq. (2.23) shows that τ is the ratio of two quadratic functions of L_2. This relation is easily inverted to get

$$L_2=\frac{-1+\alpha_1\eta+\alpha_2\eta^2+\alpha_3\eta^3+(1+2\eta)[1+\beta_1\eta+\beta_2\eta^2+\beta_3\eta^3+\beta_4\eta^4]^{1/2}}{12\eta(\gamma_0+\gamma_1\eta+\gamma_2\eta^2)}, \tag{2.25}$$

where the expressions of the coefficients α_i, β_i, and γ_i as functions of λ, A, and τ are given in Appendix A.

So far, we are free to fix τ as a function of η, x, and λ by following any criterion we wish. In particular, we can enforce Eq. (2.22), as done in Ref. 44. Analogously, the parameter $A(\eta,x,\lambda)$ (which was taken as $A=x$ in Ref. 44) can be freely chosen. In the simplified version of the model we consider here, we assume that both A and τ are *independent*

of density, so they take values needed to satisfy the requirement (2.12). Those values are simply

$$A=x, \quad \tau=[12x\lambda(\lambda-1)]^{-1}. \tag{2.26}$$

Note that this τ is only slightly different from the parameter τ_{SW} introduced below Eq. (1.1), both of them becoming identical to τ_{SHS} in the limit $\lambda\rightarrow1$. The choice (2.26) closes the construction of the model. The pair distribution function
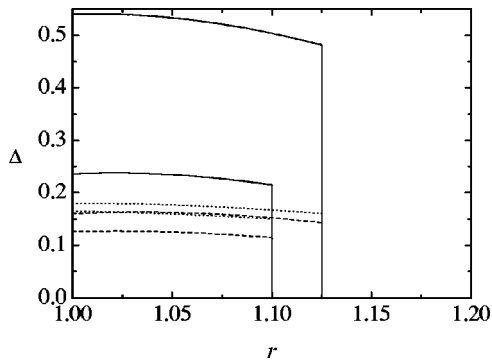
FIG. 1. Function $\Delta(r)$ defined by Eq. (2.28) for $\lambda=1.1$ and $\lambda=1.125$ and for the temperatures $T=0.5$ (solid lines), 0.67 (dashed lines), and 1 (dotted lines).

in Laplace space is given by Eqs. (2.4) and (2.16), where the expressions for the coefficients are (2.17)–(2.20), (2.25), and (2.26). The model provides the quantity $G(t)$ as an explicit function of the Laplace variable t, the packing fraction η, the well width λ, and the temperature parameter $x \equiv e^{1/T}-1$. Since the poles of $F(t)$ are the roots of a cubic equation, the inverse Laplace transforms of $t[F(t)]^n$ are analytically derived and then the radial distribution function is readily obtained from the representation (2.5). From Eq. (2.26), it follows that the relationship between the temperature and the parameter τ is

$$T = 1/\ln[1+\tau^{-1}/12\lambda(\lambda-1)]. \qquad (2.27)$$

The predictions of our model to first order in the packing fraction are compared with the exact results in Appendix B. As an illustrative example, Fig. 1 shows the quantity

$$\Delta(r) = \lim_{\eta \to 0} \frac{1}{\eta} \frac{g(r)-g_{\text{exact}}(r)}{g_{\text{exact}}(r)}, \qquad (2.28)$$

for $\lambda=1.1$ and $\lambda=1.125$ and for the temperatures $T=0.5$, 0.67, and 1. The function $\Delta(r)$ is different from zero in the interval $1<r<\lambda$ only, where our model slightly overestimates the value of $g(r)$. Note that the relative deviation of
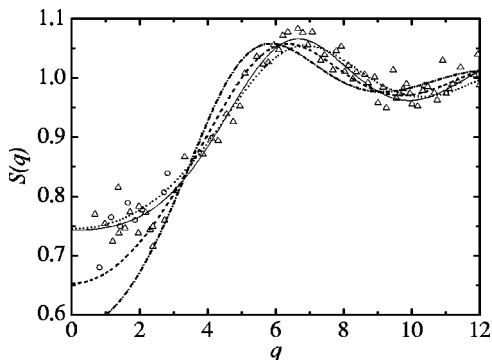

FIG. 2. Structure factor, $S(q)$, corresponding to a SW fluid with $\lambda=1.1$, $\eta=0.07$, and $T^{-1}=0.92$. The circles and triangles are MC data taken from Fig. 3 of Ref. 47. The lines are the result predicted by the present model (—), the PY equation for SHS ($\cdots$), the TL perturbation theory (- - -), and the PY equation for HS (- · - · -).

our $g(r)$ from the exact radial distribution function is $\Delta(r)\eta$ for small densities. Of course, the linear growth of this deviation with increasing density is valid in this low-density regime only, as comparison with simulation values at finite densities shows [cf. Figs. 4 and 5].

Appendix C shows that the model reduces to Wertheim–Thiele's and Baxter's analytical solutions of the PY equation in the HS and SHS limits, respectively. If we consider the parameter space $\lambda-\tau^{-1}$, then the HS potential corresponds to the line $\tau^{-1}=0$ (in which case the physical properties are independent of λ), while the SHS potential corresponds to the line $\lambda=1$ (the physical properties being τ-dependent). What our model does is to extend the above picture to the entire plane $\tau^{-1}\geq0$, $\lambda\geq1$, without compromising the mathematical simplicity present in the analytical solutions of the PY integral equation for HS and SHS.

III. COMPARISON WITH SIMULATION AND OTHER THEORIES

A. Structural properties

The structural properties obtained from the original version of the model [i.e., with L_2 determined by solving the transcendent equation stemming from Eq. (2.22)] were profusely compared with simulation data[33,41,47] in Ref. 44. We have checked that the simplified version of the model presented here [cf. (2.25), (2.26)] gives results very close to those of the original model, especially for narrow wells. Consequently, we will present only a brief comparison with simulations in this subsection.

The structure of a fluid is usually determined by neutron- or x-ray scattering experiments, which measure the structure factor $S(q)$. This quantity is directly related to the Laplace transform $G(t)$ by Eq. (2.1) and so can be obtained explicitly in our model. In 1984, Huang et al.[47] performed MC simulations of SW fluids with $\lambda=1.1$ to reproduce the main features of the structure factor of micellar suspensions. Figure 2 shows $S(q)$ obtained from simulation[47] for $\lambda=1.1$, $T^{-1}=0.92$, and $\eta=0.07$, as compared with our model, the PY solution for SHS (with the conventional choice of τ_{SW}^{-1} as the stickiness parameter), the Tang–Lu (TL) perturbation theory,[36,37] and the PY solution for hard spheres. The deviations of the simulation data from the PY–HS curve are essentially a measure of effects associated with the nonzero values of the square-well width and of the inverse temperature. These are qualitatively described by the TL perturbation theory, except for small wave numbers. This region is well represented by the PY–SHS curve and by our model, but the latter is better near the first maximum. The value of the critical temperature for $\lambda=1.1$ can be estimated to be $T_c\approx0.5$ [cf. Table I]. Consequently, the case considered in Fig. 2 corresponds to a rather hot gas. That is why the simulation data are not too far from the HS values (except in the region $q\lesssim3$). In order to highlight the differences that can be expected at a smaller temperature, the case $T=0.5$ is considered in Fig. 3. Now, the structure factor predicted by our model and by the PY–SHS solution is very different from that predicted by the TL perturbation theory, the latter being very close to the PY-HS solution. This is not surprising, since
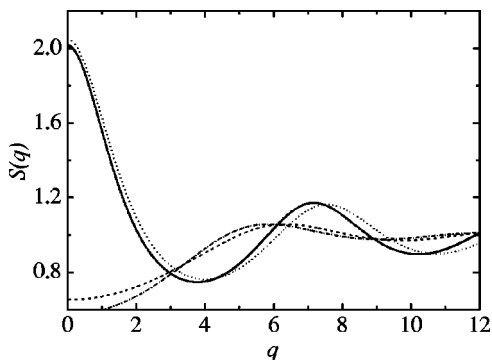
FIG. 3. Structure factor, $S(q)$, corresponding to a SW fluid with $\lambda = 1.1$, $\eta = 0.07$, and $T = 0.5$. The lines are the result predicted by the present model (——), the PY equation for SHS ($\cdots$), the TL perturbation theory (- - -), and the PY equation for HS (- · - · -).

FIG. 5. Plot of $g(1^+)$ as a function of $1/T$ for $\lambda = 1.125$ and three densities: $\rho = 0.4$ ($\bigcirc$), $\rho = 0.6$ ($\square$), and $\rho = 0.8$ ($\diamondsuit$). The symbols represent MC data taken from Ref. 33 ($1/T \neq 0$) and from Ref. 52 ($1/T = 0$). The dotted lines are the results obtained from the model of Ref. 44, the solid lines are the results given by the present model, and the dashed lines are the predictions from the TL perturbation theory.

in any perturbation theory the quantities are expanded in powers of T^{-1} and obviously the value $T^{-1} = 2$ is beyond its range of applicability. On the other hand, the curves corresponding to the PY–SHS solution and our model are relatively close (except for a slight phase shift), as expected from the fact that the well width is rather small. Moreover, since the stickiness parameter has been chosen so as to reproduce the correct second virial coefficient, the PY–SHS solution does a generally good job at this very low density.

Now, we consider the radial distribution function itself. As a representative example of a width not extremely small, we take the case $\lambda = 1.125$, for which MC simulations are available.[33] Figure 4 shows $g(r)$ for $\lambda = 1.125$ at the thermodynamic state $T = 1$, $\rho = 0.8$. As seen in the figure, the original model of Ref. 44 exhibits a remarkable agreement with the simulation data. We also observe that our present model captures reasonably well the behavior of $g(r)$ at this high density, while the TL approximation predicts a too small contact value of $g(1^+)$. The contact values are plotted in Fig. 5 as a function of $1/T$ for $\lambda = 1.125$ and $\rho = 0.4$, 0.6, and 0.8. At $1/T = 0$ the system corresponds to HS and then our model and the TL theory reduce to Wertheim–Thiele's solution of the PY equation, which tends to underestimate $g(1^+)$ at high densities. As the inverse temperature increases, the TL theory
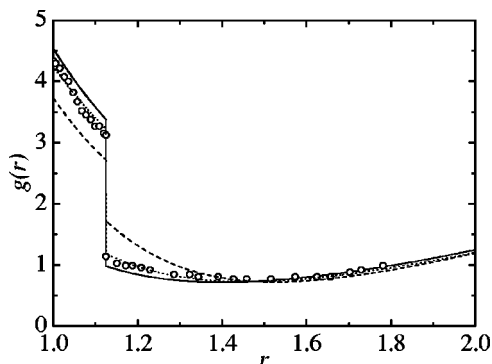
predicts a linear increase of $g(1^+)$ [cf. Eq. (1.2)] that clearly deviates from the MC data. On the other hand, the temperature dependence of $g(1^+)$ is well described by both the original and the simplified versions of the model, except at $1/T = 2$.

B. Thermodynamic properties

The compressibility equation of state is obtained from Eqs. (2.3) and (A1). This route is preferable to the virial route because the latter is known to yield an unphysical critical behavior in the SHS limit.[53] From Eq. (2.3), we have

$$Z(\eta, T) \equiv \frac{p}{\rho k_B T} = \eta^{-1} \int_0^\eta d\eta' \, \chi_T^{-1}(\eta', T), \qquad (3.1)$$

where the density dependence of χ_T is given in our model by Eqs. (A1) and (2.25). Although this dependence is known explicitly, it does not allow us to perform the integration in Eq. (3.1) analytically, so the compressibility factor Z is obtained by numerical integration.

Before delving into the thermodynamic predictions of our model, let us compare it with the original one[44] in the case of a moderately narrow well, namely $\lambda = 1.125$. Figure 6 shows the density dependence of the inverse susceptibility for $T = 0.5$, 0.67, and 0.9. As the temperature increases, our simplified model is seen to overestimate the compressibility of the fluid, especially for large densities. On the other hand, at $T = 0.5$ (which is practically the critical temperature, cf. Table I), both versions of the model yield undistinguishable results. This is quite encouraging, since it is in the domain of low temperatures (or, equivalently, high stickiness) where our model is expected to correct the deficiencies of perturbation theories and become useful.

One of the advantages of our simplified model is that it allows us to derive explicit expressions for the coordinates of the critical point. The spinodal line is the locus of points where the isothermal compressibility diverges. Equation (A1) clearly shows that $\chi_T = S(0) \to \infty$ if and only if $L_2 \to \infty$. Thus, according to Eq. (2.25), the spinodal line is

FIG. 4. Radial distribution function, $g(r)$, corresponding to a SW fluid with $\lambda = 1.125$, $\rho = 0.8$, and $T = 1$. The circles represent MC data (Ref. 33), the dotted line is the result obtained from the model of Ref. 44, the solid line is the result given by the present model, and the dashed line is the prediction from the TL perturbation theory.
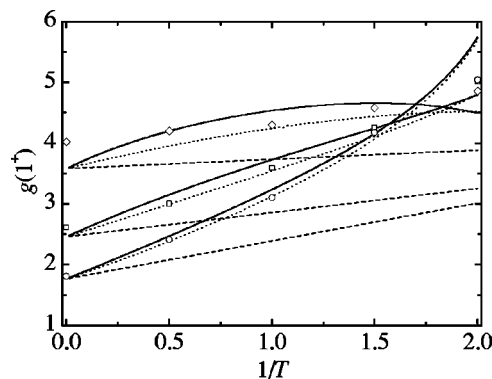
J. Chem. Phys., Vol. 115, No. 6, 8 August 2001

Square-well model for colloidal systems   2811

given by a solution to the quadratic equation $\gamma_0 + \gamma_1 \eta + \gamma_2 \eta^2 = 0$. This equation has two real solutions, $\eta_\pm(\tau)$, only if τ is a smaller than a critical value τ_c given by

$$\tau_c^{-1} = 12 \frac{3 + \lambda + 2\sqrt{2\lambda}}{9 - 2\lambda + \lambda^2}. \tag{3.2}$$

The critical temperature T_c is obtained by setting $\tau = \tau_c$ in Eq. (2.27). If $\tau < \tau_c$, the smallest root, $\eta_-(\tau)$, does not define the vapor branch of the spinodal line because it is also a root of the numerator of Eq. (2.25), and so L_2 remains finite at $\eta = \eta_-(\tau)$. Therefore, only the liquid branch of the spinodal line, $\eta_+(\tau)$, exists. It is given by

$$\eta_+(T) = \frac{(1 + \lambda + \lambda^2)\sqrt{1 - \frac{1}{6}(3 + \lambda)\tau^{-1} + \frac{1}{144}(9 - 2\lambda + \lambda^2)\tau^{-2}} + \frac{1}{12}(3 + \lambda^3)\tau^{-1} - 1 - \lambda + \lambda^2}{\lambda[\frac{1}{3}(2 + 3\lambda + \lambda^2 + \lambda^3)\tau^{-1} - 4\lambda]}. \tag{3.3}$$

The critical density is $\eta_c = \eta_+(\tau_c)$, i.e.,

$$\eta_c = \frac{\frac{1}{12}(3 + \lambda^3)\tau_c^{-1} - 1 - \lambda + \lambda^2}{\lambda[\frac{1}{3}(2 + 3\lambda + \lambda^2 + \lambda^3)\tau_c^{-1} - 4\lambda]}. \tag{3.4}$$

As λ increases, T_c increases, while η_c decreases. Equations (3.2)–(3.4) generalize to $\lambda > 1$ the results predicted by the PY solution for SHS[7]

$$\eta_+ = \frac{\sqrt{9 - 6\tau^{-1} + \tau^{-2}/2} + \tau^{-1} - 3}{7\tau^{-1} - 12},$$

$$\tau_c^{-1} = 3(2 + \sqrt{2}) \simeq 10.24, \quad \eta_c = \frac{3}{2}\sqrt{2} - 2 \simeq 0.1213. \tag{3.5}$$

The lack of a vapor branch of the spinodal line is a feature that our model inherits from the PY–SHS solution.[53] Our model also has in common with the SHS limit, as well as with the solution of the PY equation for finite λ,[54] the existence of regions in the temperature–density plane, inside which the physical quantities cease to take real values. According to Eq. (2.25), this happens when $1 + \beta_1 \eta + \beta_2 \eta^2 + \beta_3 \eta^3 + \beta_4 \eta^4 < 0$. Let us call $\eta_i(T)$ ($i = 1, \ldots, 4$) the four roots of the quartic equation $1 + \beta_1 \eta + \beta_2 \eta^2 + \beta_3 \eta^3 + \beta_4 \eta^4 = 0$, with the convention that, whenever they are real, $\eta_1 \leq \eta_2 \leq \eta_3 \leq \eta_4$. It turns out that the roots $\eta_1(T)$ and $\eta_2(T)$ are real only if τ is smaller than a certain threshold value τ_{th} (or, equivalently, if $T < T_{th}$); they define a dome-shaped curve with an apex at a density $\eta_{th} = \eta_1(T_{th}) = \eta_2(T_{th})$. Analogously, the other two roots, $\eta_3(T)$ and $\eta_4(T)$, are real only if $\tau < \tau'_{th}$ ($T < T'_{th}$) and define another dome-shaped curve with an apex at $\eta'_{th} = \eta_3(T'_{th}) = \eta_4(T'_{th})$. Consequently, the parameter L_2 becomes complex inside the intervals $\eta_1(T) < \eta < \eta_2(T)$ (for $T < T_{th}$) and $\eta_3(T) < \eta < \eta_4(T)$ (for $T < T'_{th}$). However, the existence of the second region is a mathematical artifact since it affects unphysically high densities. For instance, for $\lambda = 1.125$ we have $T'_{th} = 0.535\,147$ and $\eta'_{th} = 0.786\,92$, this density being larger than the one corresponding to the close packing value $\eta_{cp} = \sqrt{2}\pi/6 \simeq 0.740$. In fact, in the SHS limit ($\lambda \to 1$) the second region collapses into the line $\eta = 1$ and disappears. On the other hand, the region $\eta_1(T) < \eta < \eta_2(T)$ is inside the curve $\eta = \eta_\pm(T)$ and persists in the SHS limit. In the latter case, the threshold values coincide with the critical ones, i.e., $\tau_{th} = \tau_c$, $\eta_{th} = \eta_c$. For finite λ, T_{th} is smaller but practically

indistinguishable from T_c and η_{th} is slightly smaller than η_c. In the illustrative case of $\lambda = 1.125$, we have $T_c = 0.502\,324$, $\eta_c = 0.112\,99$, $T_{th} = 0.502\,269$, and $\eta_{th} = 0.109\,80$. The existence line, $\rho = \rho_{1,2}(T)$, and the liquid branch of the spinodal line, $\rho = \rho_+(T)$, are shown in Fig. 7 for $\lambda = 1.125$.

Recently, it has been suggested[55] that, while the critical point is in general very sensitive to the range of the interaction, the second virial coefficient has a fairly constant value at the critical temperature, $B_2(T_c) \approx -\pi$. In the case of the SW interaction, computer simulations[48,56] show that the value of the second virial coefficient $B_2(T) = -2\pi[x(\lambda^3 - 1) - 1]/3$ at $T = T_c$ is much less sensitive to the width λ than the critical temperature.[26,55] Moreover, the PY–SHS solution predicts $B_2(T_c) = -(2 + 3\sqrt{2})\pi/6 \approx -1.04\pi$. Thus, by assuming that $B_2(T_c)$ is independent of λ and is equal to its value in the SHS limit, the criterion of Ref. 55 allows one to estimate the critical temperature as

$$T_c = 1/\ln[1 + 3(2 + \sqrt{2})/4(\lambda^3 - 1)]. \tag{3.6}$$

Since the model presented in this paper is constructed as a simple generalization of Baxter's solution of the PY equation for SHS, we expect its predictions for the critical values of the temperature (T_c), the density (ρ_c), and the compress-
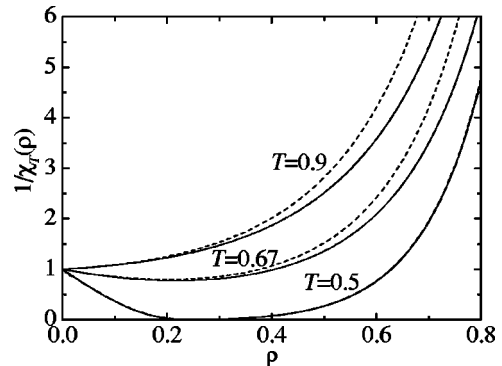

FIG. 6. Density dependence of the inverse isothermal susceptibility for $\lambda = 1.125$ and three temperatures. The dashed lines are the results obtained from the model of Ref. 44 and the solid lines are the results from the present model.

2812   J. Chem. Phys., Vol. 115, No. 6, 8 August 2001

L. Acedo and A. Santos

TABLE I. Critical constants of the square-well fluid for several values of the width parameter λ.

λ	T_c	ρ_c	Z_c	Source
1	0^a	0.232	0.379	PY equation (Ref. 7)
1.1	0.455	0.219	0.372	This work
	0.461			Eq. (3.6) (Ref. 55)
1.125	0.502	0.216	0.370	This work
	0.512			Eq. (3.6) (Ref. 55)
	0.594	0.46	0.42	Perturbation theory (Ref. 33)
	0.587	0.71	0.74	Perturbation theory (Ref. 34)
1.25	0.764	0.370	0.29	Computer simulation (Ref. 48)
	0.729	0.203	0.360	This work
	0.766			Eq. (3.6) (Ref. 55)
	0.913	0.34	0.43	Perturbation theory (Ref. 33)
	0.850	0.48	0.47	Perturbation theory (Ref. 34)
1.375	0.974	0.355	0.30	Computer simulation (Ref. 48)
	0.960	0.193	0.349	This work
	1.046			Eq. (3.6) (Ref. 55)
	1.11	0.34	0.39	Perturbation theory (Ref. 33)
	1.08	0.36	0.40	Perturbation theory (Ref. 34)
1.5	1.219	0.299	0.30	Computer simulation (Ref. 48)
	1.209	0.184	0.339	This work
	1.367			Eq. (3.6) (Ref. 55)
	1.205	0.200	0.37	PY equation (Ref. 54)
	1.35	0.31	0.36	Perturbation theory (Ref. 33)
	1.33	0.29	0.37	Perturbation theory (Ref. 34)
1.625	1.479	0.177	0.330	This work
	1.738			Eq. (3.6) (Ref. 55)
	1.70	0.27	0.38	Perturbation theory (Ref. 33)
	1.61	0.26	0.36	Perturbation theory (Ref. 34)
1.75	1.811	0.284	0.35	Computer simulation (Ref. 48)
	1.777	0.170	0.322	This work
	2.164			Eq. (3.6) (Ref. 55)
	2.04	0.25	0.38	Perturbation theory (Ref. 33)
	1.93	0.24	0.36	Perturbation theory (Ref. 34)
1.85	2.036	0.165	0.317	This work
	2.550			Eq. (3.6) (Ref. 55)
	2.33	0.25	0.37	Perturbation theory (Ref. 33)
	2.23	0.23	0.35	Perturbation theory (Ref. 34)
2	2.764	0.225	0.32	Computer simulation (Ref. 48)
	2.466	0.159	0.310	This work
	3.208			Eq. (3.6) (Ref. 55)
	2.88	0.24	0.37	Perturbation theory (Ref. 33)
	2.79	0.23	0.35	Perturbation theory (Ref. 34)

$^a\tau_c=0.0976$.
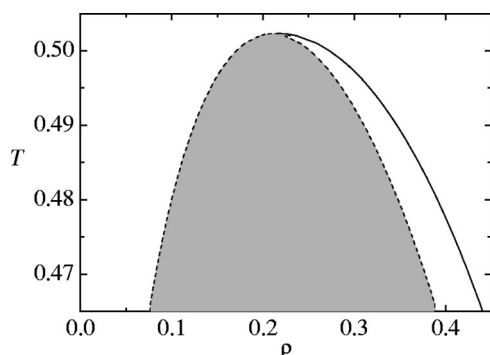
FIG. 7. Liquid branch of the spinodal line (solid line) and existence line (dashed line) for $\lambda=1.125$, according to the present model. The model does not give real values for the physical quantities inside the gray region enclosed by the existence line.
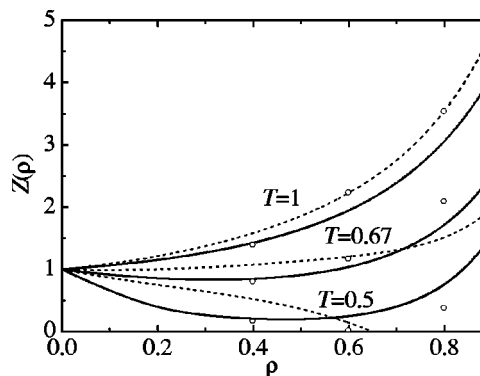
FIG. 8. Density dependence of the compressibility factor for $\lambda=1.125$ and three temperatures. The circles are the results of computer simulations (Ref. 33), the solid lines are the results from our model, and the dashed lines are the TL perturbation theory predictions (Ref. 37).

ibility factor (Z_c) to be more reliable for small values of $\lambda-1$ than for wide wells. However, to the best of our knowledge, the simulation estimates for those quantities are only available for $\lambda \geq 1.25$,[48] and so we cannot make a comparison for smaller widths. Table I shows the values of T_c, ρ_c, and Z_c for several values of λ, as estimated from computer simulations,[48] and as predicted by the model, by Eq. (3.6), by perturbation theory,[33,34] and by the PY integral equation.[54]

Comparison with MC simulation data shows that the critical temperature predicted by our model, Eq. (3.2), tends to be smaller than the correct value, while Vliegenthart and Lekkerkerker's criterion,[55] as well as second-order perturbation theory[33,34] tend to overestimate it. What is indeed remarkable is the fact that Eq. (3.2) provides the best agreement with computer simulations for $\lambda \leq 1.75$ [except at $\lambda=1.25$, in which case Eq. (3.6) is better]. In the case of the critical value of the compressibility factor, the best agreement corresponds to our model, except at $\lambda=1.75$, where Chang and Sandler's perturbation theory gives a better result. On the other hand, the critical densities predicted by our model are around 30%–45% smaller than the simulation values, a discrepancy that can be traced back to the solution of the PY equation for SHS. Since the computer simulations and all the theories share the property that ρ_c is a monotonically decreasing function of λ, we can conclude that the correct value of ρ_c in the limit $\lambda \to 1$ is certainly larger than the simulation value $\rho_c=0.370$ at $\lambda=1.25$, while Baxter's solution yields $\rho_c=0.232$. Thus, we can expect this failure to reproduce accurately the critical density also present in the PY approximation for finite λ. This is confirmed by the results of a numerical solution of the PY equation for $\lambda=1.5$,[54] which gives a value of ρ_c rather close to the one obtained here.

Now, let us compare the general density dependence of the compressibility factor predicted by the model with available computer simulations. We start with the smallest value of λ that, to our knowledge, has been analyzed in simulations, namely $\lambda=1.125$.[33] Figure 8 shows $Z(\rho)$ for $\lambda=1.125$ and $T=0.5$, 0.67, and 1. Strictly speaking, the curve representing the model at the lowest temperature corresponds to $T=T_c \approx 0.502$ rather than to $T=0.5$. This is because at $T=0.5$ there exists a small density interval around ρ_c
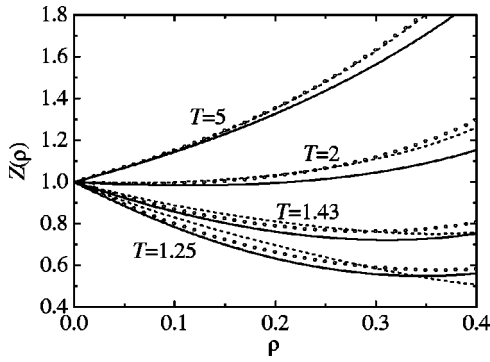
FIG. 9. Density dependence of the compressibility factor for $\lambda = 1.4$ and four temperatures. The circles correspond to an empirical formula fitted to molecular dynamics results (Ref. 49), the solid lines are the results from the present model, and the dashed lines are the TL perturbation theory predictions (Ref. 37).

≈ 0.22 [cf. Fig. 7] where the model gives complex values. The next width we consider is $\lambda = 1.4$, for which extensive molecular dynamics simulations are available.[49] The results for $T = 1.25$, 1.43, 2, and 5 are plotted in Fig. 9. We observe that, except at the highest temperatures ($T = 1$ for $\lambda = 1.125$, $T \geq 2$ for $\lambda = 1.4$), our model presents a better general agreement with the simulation data than the TL perturbation theory.

IV. CONCLUDING REMARKS

The main objective of this paper has been to propose an analytical model that could be useful to describe the structural and thermodynamic properties of systems, such as colloidal dispersions, composed of particles effectively interacting through a hard-core potential with a short-range attraction. As the simplest interaction that captures both features, we have considered the square-well (SW) potential (1.1). On the one hand, perturbation theory becomes unreliable when the range $\lambda - 1$ of the attraction is small, especially at low temperatures, i.e., when a certain degree of ''stickiness'' among the particles becomes important. On the other hand, the widely used sticky-hard-sphere (SHS) interaction model combines temperature and well width in one parameter only, thus lacking the flexibility to accommodate additional changes in width and/or temperature. Our approach intends to fill the gap between these two theories.

The model presented in this paper is based on the one proposed in Ref. 44, where the functions $R(t)$ and $\bar{R}(t)$ defined by Eqs. (2.4) and (2.13) were approximated by rational forms, Eq. (2.14). The parameters in these functions are constrained to yield a finite value for the isothermal compressibility by Eqs. (2.17)–(2.20). This still leaves two free parameters, A and τ, the latter being defined in Eq. (2.23), as unknown functions of the packing fraction η, the temperature parameter $x \equiv e^{1/T^*} - 1$, and the well width λ. Apart from their zero-density limits (2.21) and (2.24), two extra conditions are needed to fix those parameters and close the construction of the model. Thus, depending on the physical situation one is interested in and/or on the degree of simplicity one wants to keep in the model, it is possible to choose different criteria to determine A and τ. For instance, one

could impose certain continuity conditions on the cavity function $y(r) \equiv g(r) e^{\varphi(r)/k_B T}$ at the points where the potential is singular;[51] alternatively, one could require thermodynamic consistency among the virial, compressibility, and energy routes. Of course, other choices are possible. In the original formulation of the model, A was assumed to be independent of density (hence, $A = x$) and the second condition was the continuity of $y(r)$ at $r = \lambda \sigma$, giving rise to a transcendent equation that needed to be solved numerically. On the other hand, in this paper we have simply assumed that both A and τ are independent of density, Eq. (2.26). The assumption for τ is expected to be especially adequate for narrow potentials, since in the SHS limit the role of τ is played by the parameter $\tau_{SHS} = [12x(\lambda - 1)]^{-1}$, which is indeed independent of density. With these choices for A and τ the problem remains fully algebraic and all the parameters can be expressed in terms of the solution of a quadratic equation, in analogy with what happens in Baxter's solution of the PY equation for SHS.[7] In fact, the model includes such a solution as a limit case. Given the scarcity of simulation results for narrow wells, we have been forced to carry out a comparison for cases with $\lambda \geq 1.125$. In spite of that, the results show a very good general performance of the structural and thermodynamic properties predicted by the model, correcting the inadequacy of the perturbation theory predictions in the low-temperature domain. It is interesting to note that the model provides an explicit expression of the critical temperature as a function of the well width, Eq. (3.2), which is accurate even for rather wide wells.

The results of this paper could also be useful in connection with a recently proposed extension of the law of corresponding states for systems, such as colloidal suspensions, that have widely different ranges of attractive interactions.[26] Given an interaction potential $\varphi(r) = \varphi_{\text{rep}}(r) + \varphi_{\text{att}}(r)$, where φ_{rep} and φ_{att} are the repulsive (not necessarily hard-core) and attractive parts, respectively, one can define a (temperature-dependent) effective hard-core diameter,

$$\sigma = \int_0^{\infty} dr \, [1 - e^{-\varphi_{\text{rep}}(r)/k_B T}], \qquad (4.1)$$

an effective well depth,

$$\epsilon = -\varphi(r_0), \qquad \left. \frac{d\varphi(r)}{dr} \right|_{r=r_0} = 0, \qquad (4.2)$$

and a (temperature-dependent) effective well width,

$$\lambda = [1 + (B_2^* - 1)(1 - e^{\epsilon/k_B T})^{-1}]^{1/3}, \qquad (4.3)$$

where

$$B_2^* = \frac{3}{\sigma^3} \int_0^{\infty} dr \, r^2 [1 - e^{-\varphi(r)/k_B T}], \qquad (4.4)$$

is the reduced second virial coefficient. Then, according to the extended law of corresponding states,[26] the compressibility factor for a wide range of colloidal materials is a function of only the reduced temperature $T^* = k_B T/\epsilon$, the reduced density $\rho^* = \rho \sigma^3$, and the range parameter λ, i.e., $Z = F(T^*, \rho^*, \lambda)$, where the function F is hardly sensitive to the details of the potential. As a consequence, an accurate
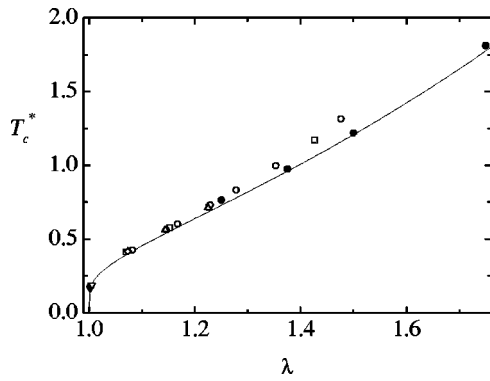
FIG. 10. Dependence of the reduced critical temperature on the effective well width, as obtained from computer simulations for several interaction potentials: square-well (solid circles) (Ref. 48), hard-core Yukawa (open squares) (Refs. 26,57,58), generalized Lennard-Jones (open circles) (Refs. 26,59), α-Lennard-Jones (open diamond) (Refs. 26,60), an effective colloid–colloid interaction (up triangles) (Refs. 26,61), and an effective interaction for nonadditive mixtures of asymmetric hard spheres (down triangles) (Refs. 26,62,63). The solid line is the prediction of our model, Eqs. (2.27) and (3.2).

prescription for the function F based on the SW interaction for variable width can be used to determine the thermodynamic properties of a wide class of colloidal suspensions. As an illustrative example, Fig. 10 shows the dependence of the reduced critical temperature $T_c^* = k_B T_c/\epsilon$ on the effective width λ for several interaction potentials.[26] The prediction of our model, Eqs. (2.27) and (3.2), is also plotted. The extended law of corresponding states work very well up to $\lambda \lesssim 1.3$. For larger interaction ranges the values of T_c^* for the generalized Lennard-Jones and the hard-core Yukawa potentials tend to lie slightly above those corresponding to the SW interaction.

In the near future, we plan to extend the model presented in this paper in two directions. First, the case of a mixture of particles interacting through SW potentials with different values of σ, ϵ, and λ will be analyzed. This generalization must be such that one recovers the cases of a mixture of hard spheres,[64] a mixture of sticky hard spheres,[65] and a monodisperse SW system in the appropriate limits. As a second extension, we will study the case of an interaction model made of a hard core plus a square shoulder plus a square well, for which, in addition to the conventional gas–liquid phase transition, a liquid–liquid transition in the supercooled phase appears.[66–68]

ACKNOWLEDGMENTS

APPENDIX A: SOME EXPLICIT EXPRESSIONS

1. Expression for $S(0)$

In this Appendix we list some of the expressions that are derived from the model. The long-wavelength value of the structure factor is obtained by using the model (2.16) in the general expression (2.10). The result is

$$S(0) = \frac{1}{5(1+2\eta)^2}\{5 - 20\eta[1+(2+\lambda)A'-3(1+\lambda)L_2] + 2\eta^2[15 - 6(14-\lambda+19\lambda^2-\lambda^3-\lambda^4)L_2 + 120(1+\lambda+\lambda^2)L_2^2$$

$$+ (50+16\lambda+27\lambda^2-2\lambda^3-\lambda^4)A' - 30(5+4\lambda+3\lambda^2)A'L_2$$

$$+ 15(3+2\lambda+\lambda^2)A'^2] - 2\eta^3[10+3(7-53\lambda-13\lambda^2+7\lambda^3-8\lambda^4)L_2 - 60(1+\lambda)(1-4\lambda+\lambda^2)(1+\lambda+\lambda^2)L_2^2$$

$$+ (19+59\lambda+9\lambda^2-\lambda^3+4\lambda^4)A' + 3(11-67\lambda-114\lambda^2-66\lambda^3-13\lambda^4+9\lambda^5)A'L_2 + 3(3+2\lambda+\lambda^2)(1+7\lambda+3\lambda^2$$

$$- \lambda^3)A'^2] + \eta^4[5 - 12(1+\lambda+\lambda^2+11\lambda^3-4\lambda^4)L_2 + 240\lambda^3(1+\lambda+\lambda^2)L_2^2 + 2(7+8\lambda+9\lambda^2+10\lambda^3-4\lambda^4)A'$$

$$- 12(1+3\lambda+6\lambda^2+24\lambda^3+17\lambda^4+9\lambda^5)A'L_2 + 3(3+2\lambda+\lambda^2)(1+2\lambda+3\lambda^2+4\lambda^3)A'^2]\}, \tag{A1}$$

where we have made use of Eqs. (2.17)–(2.20).

2. Expressions for the coefficients in Eq. (2.25)

Equation (2.23) reduces to a quadratic equation for L_2. Its physical solution is given by Eq. (2.25), where

$$\alpha_1 = 2A'(2+\lambda) + \tfrac{1}{6}(1+4\lambda+\lambda^2-3A')\tau^{-1}, \tag{A2}$$

$$\alpha_2 = 3 + A'(7+2\lambda-3\lambda^2) - \tfrac{1}{12}[7+\lambda+16\lambda^2+A'(23+15\lambda+15\lambda^2+7\lambda^3)]\tau^{-1}, \tag{A3}$$

$$\alpha_3 = -2 - 2A'(1+2\lambda+3\lambda^2) + \tfrac{1}{6}[7+\lambda-2\lambda^2+A'(7+15\lambda+21\lambda^2+11\lambda^3+6\lambda^4)]\tau^{-1}, \tag{A4}$$

$$\beta_1 = -4 - 4A'(2+\lambda) + \tfrac{1}{3}(5+2\lambda-\lambda^2+3A')\tau^{-1} - \tfrac{1}{3}\tau^{-2}, \tag{A5}$$

$$\beta_2 = 6 + 6A'(3+2\lambda+\lambda^2) + 4A'^2(2+\lambda)^2 - \tfrac{1}{6}[9(3+\lambda) + A'(59+51\lambda+3\lambda^2-5\lambda^3) + 12A'^2(2+\lambda)]\tau^{-1} + \tfrac{1}{36}[31+8\lambda$$

$$+ 18\lambda^2-4\lambda^3+\lambda^4+12A'(5+\lambda)+9A'^2]\tau^{-2}, \tag{A6}$$

$$\beta_3 = -4 - 12A'(1+\lambda+\lambda^2) - 4A'^2(2+\lambda)(1+2\lambda+3\lambda^2) + \tfrac{1}{3}[3(4+\lambda+\lambda^2) + A'(29+36\lambda+30\lambda^2+7\lambda^3-3\lambda^4) + A'^2(17$$
$$+ 43\lambda + 30\lambda^2 + \lambda^3 - \lambda^4)]\tau^{-1} - \tfrac{1}{36}[29 + 13\lambda + 27\lambda^2 + 7\lambda^3 - 4\lambda^4 + A'(68 + 80\lambda + 80\lambda^2 + 16\lambda^3 + 7\lambda^4 + \lambda^5)$$
$$+ 3A'^2(13 + 13\lambda + \lambda^2 - 3\lambda^3)]\tau^{-2}, \tag{A7}$$

$$\beta_4 = [1 + A'(1+2\lambda+3\lambda^2)]^2 \tfrac{1}{6}[7 + \lambda + 4\lambda^2 + 2A'(7$$
$$+ 15\lambda + 15\lambda^2 + 5\lambda^3 + 6\lambda^4) + A'^2(1+2\lambda+3\lambda^2)(7$$
$$+ 15\lambda + 3\lambda^2 - \lambda^3)]\tau^{-1} + \tfrac{1}{144}[49 + 38\lambda + 9\lambda^2 + 8\lambda^3$$
$$+ 16\lambda^4 + 2A'(49 + 88\lambda + 112\lambda^2 + 80\lambda^3 + 35\lambda^4$$
$$- 4\lambda^5) + A'^2(49 + 138\lambda + 219\lambda^2 + 124\lambda^3 + 27\lambda^4$$
$$+ 18\lambda^5 + \lambda^6)]\tau^{-2}, \tag{A8}$$

$$\gamma_0 = 1 + \lambda - \tfrac{1}{6}\tau^{-1}, \tag{A9}$$

$$\gamma_1 = 2(1 + \lambda - \lambda^2) - \tfrac{1}{6}(3+\lambda^3)\tau^{-1}, \tag{A10}$$

$$\gamma_2 = \lambda[-4\lambda + \tfrac{1}{3}(2+3\lambda+\lambda^2+\lambda^3)\tau^{-1}]. \tag{A11}$$

The other root is incompatible with (2.21) and then must be discarded.

APPENDIX B: LOW-DENSITY BEHAVIOR OF THE MODEL

In the low-density limit, Eqs. (2.17)–(2.20) become, respectively,

$$L_1 = 1 - \tfrac{3}{2}\eta[1 - x(\lambda^4-1)] + \mathcal{O}(\eta^2), \tag{B1}$$

$$S_1 = \mathcal{O}(\eta), \tag{B2}$$

$$S_2 = -\tfrac{1}{2}[1 - x(\lambda^2-1)] + \mathcal{O}(\eta), \tag{B3}$$

$$S_3 = -\frac{1}{12\eta} + \frac{1}{3}[1 - x(\lambda^3-1)] + \mathcal{O}(\eta). \tag{B4}$$

To first order in density, Eq. (2.25) gives

$$L_2 = x\lambda(\lambda-1) + L_2^{(1)}\eta + \mathcal{O}(\eta^2), \tag{B5}$$

where

$$L_2^{(1)} = -\tfrac{3}{2}x\lambda(\lambda-1)\{1 + x(\lambda-1)^2[1 - 2\lambda - \lambda^2$$
$$- 4x\lambda(1+\lambda)]\}. \tag{B6}$$

Substitution into Eq. (2.16) yields, after some algebra,

$$F(t) = F_{\text{exact}}(t) + \left\{ \left[\frac{2C_2}{t^4} + \frac{C_1}{t^3} + \frac{C_0}{t^2} - \left[\frac{2C_2}{t^4} \right. \right.$$
$$+ \frac{C_1 + 2C_2(\lambda-1)}{t^3}$$
$$\left. \left. + \frac{C_0 + C_1(\lambda-1) + C_2(\lambda-1)^2}{t^2} \right] e^{-(\lambda-1)t} \right] \eta \right\}$$
$$+ \mathcal{O}(\eta^2), \tag{B7}$$

where we have called

$$C_2 \equiv -3x(1+x)(\lambda^2-1), \tag{B8}$$

$$C_1 \equiv 2x(1+x)(\lambda-1)^2(1+2\lambda), \tag{B9}$$

$$C_0 \equiv \frac{L_2^{(1)}}{\lambda-1} - \frac{1}{2}x(2 - 8\lambda^3 + 3\lambda^4) - 2x^2(\lambda-1)^2$$
$$\times (2 + 4\lambda + 3\lambda^2) - 3x^3(\lambda^2-1)^2. \tag{B10}$$

The expression for the exact radial distribution function, $g_{\text{exact}}(r)$, to first order in density was derived by Barker and Henderson for the case $\lambda < 2$.[45] The corresponding expression for $F_{\text{exact}}(t)$ can be found in Ref. 44. From Eq. (B7), one easily gets

$$g(r) - g_{\text{exact}}(r) = \frac{1}{r}[C_2(r-1)^2 + C_1(r-1) + C_0]$$
$$\times [\Theta(r-1) - \Theta(r-\lambda)]\eta + \mathcal{O}(\eta^2). \tag{B11}$$

Thus, the difference (to first order in density) is nonzero in the interval $1 > r > \lambda$ only. In particular

$$g(1^+) - g_{\text{exact}}(1^+) = C_0\eta + \mathcal{O}(\eta^2), \tag{B12}$$

where[45]

$$g_{\text{exact}}(1^+) = 1 + x + \left[\frac{5}{2} + \frac{x}{2}(15 - 16\lambda^3 + 6\lambda^4) \right.$$
$$- 2x^2(\lambda-1)(4 + 4\lambda + \lambda^2 - 3\lambda^3)$$
$$\left. + 3x^3(\lambda^2-1)^2 \right]\eta + \mathcal{O}(\eta^2). \tag{B13}$$

Note that the relative coefficient $C_0/(1+x)$ vanishes in the SHS limit. As mentioned in Sec. II, the model presented in this paper does not enforce the verification of Eq. (2.22). In fact, Eq. (B11) implies that

$$g(\lambda^-) - (1+x)g(\lambda^+)$$
$$= \lambda^{-1}[C_2(\lambda-1)^2 + C_1(\lambda-1) + C_0]\eta + \mathcal{O}(\eta^2)$$
$$= \frac{x(\lambda-1)}{2\lambda}[\lambda(11 - \lambda - \lambda^2)$$
$$- x(\lambda-1)(\lambda+2)(3 + 10\lambda - 3\lambda^2)$$
$$+ 6x^2(\lambda-1)^2(1 + 3\lambda + 2\lambda^2)]\eta + \mathcal{O}(\eta^2). \tag{B14}$$

Finally, from Eq. (A1) or, equivalently, inserting Eq. (B11) into Eq. (2.1), we get

$$S(0) - S_{\text{exact}}(0) = 2x(\lambda-1)^2[7+23\lambda+30\lambda^2-4\lambda^3-2\lambda^4$$
$$-x(\lambda-1)(25+84\lambda+78\lambda^2+2\lambda^3-9\lambda^4)$$
$$+18x^2(\lambda^2-1)^2(1+2\lambda)]\eta^2+\mathcal{O}(\eta^3),$$

$$\text{(B15)}$$

where

$$S_{\text{exact}}(0) = 1 - 8[1-x(\lambda^3-1)]\eta+2[17-x(\lambda-1)(19$$
$$+19\lambda+19\lambda^2+51\lambda^3-3\lambda^4-3\lambda^5)-2x^2(\lambda$$
$$-1)^2(8+16\lambda-3\lambda^2-38\lambda^3-19\lambda^4)$$
$$+18x^3(\lambda^2-1)^3]\eta^2+\mathcal{O}(\eta^3).$$

$$\text{(B16)}$$

APPENDIX C: THE HARD-SPHERE AND STICKY-HARD-SPHERE LIMITS

1. Hard spheres

The SW potential becomes equivalent to the HS potential if $\lambda=1$ at any nonzero temperature T or if $T\to\infty$ at any width λ. Let us first consider the latter limit. Making $x=0$ in Eqs. (A2)–(A11), one gets

$$\alpha_1=0, \quad \alpha_2=3, \quad \alpha_3=-2, \tag{C1}$$

$$\beta_1=-4, \quad \beta_2=6, \quad \beta_3=-4, \quad \beta_4=1, \tag{C2}$$

$$\gamma_0=1+\lambda, \quad \gamma_1=2(1+\lambda-\lambda^2), \quad \gamma_3=-4\lambda^2. \tag{C3}$$

As a consequence, Eq. (2.25) implies that $L_2=0$. Thus, Eq. (2.16) becomes

$$F(t) = -\frac{1}{12\eta}\frac{1+L_1 t}{1+S_1 t+S_2 t^2+S_3 t^3}, \tag{C4}$$

with

$$L_1 = \frac{1+\frac{1}{2}\eta}{1+2\eta}, \tag{C5}$$

$$S_1 = -\frac{3}{2}\frac{\eta}{1+2\eta}, \tag{C6}$$

$$S_2 = -\frac{1}{2}\frac{1-\eta}{1+2\eta}, \tag{C7}$$

$$S_3 = -\frac{(1-\eta)^2}{12\eta(1+2\eta)}. \tag{C8}$$

This is precisely the form adopted by $F(t)$ in the analytical solution of the PY equation for hard spheres.[1,2,39,40] The expression for $S(0)$, Eq. (A1), simply reduces to

$$S(0) = \frac{(1-\eta)^4}{(1+2\eta)^2}. \tag{C9}$$

The case $\lambda=1$ is not considered in this subsection, as it is a particular case of the SHS limit.

2. Sticky hard spheres

Let us now take the limit $x\to\infty$, $\lambda\to1$, with $x(\lambda-1)$ = finite in the model proposed in this paper. In that limit the parameter τ is finite, cf. Eq. (2.26), while $A'=0$. Equations (A2)–(A11) become

$$\alpha_1=\tau^{-1}, \quad \alpha_2=3-2\tau^{-1}, \quad \alpha_3=-2+2\tau^{-1}, \tag{C10}$$

$$\beta_1=-4+2\tau^{-1}-\tfrac{1}{3}\tau^{-2}, \quad \beta_2=6-6\tau^{-1}+\tfrac{3}{2}\tau^{-2}, \tag{C11}$$
$$\beta_3=-4+6\tau^{-1}-2\tau^{-2}, \quad \beta_4=1-2\tau^{-1}+\tfrac{5}{6}\tau^{-2},$$

$$\gamma_0=2-\tfrac{1}{6}\tau^{-1}, \quad \gamma_1=2-\tfrac{2}{3}\tau^{-1}, \quad \gamma_3=-4+\tfrac{7}{3}\tau^{-1}. \tag{C12}$$

Therefore, Eq. (2.25) reduces to

$$L_2 = \frac{1-\eta}{24\eta}\frac{(1+2\eta)[(1-\eta)^2+2\eta(1-\eta)\tau^{-1}-\tfrac{1}{6}\eta(2-5\eta)\tau^{-2}]^{1/2}-(1-\eta)(1+2\eta-\eta\tau^{-1})}{(1-\eta)(1+2\eta)-\tfrac{1}{12}(1+4\eta-14\eta^2)\tau^{-1}}. \tag{C13}$$

Taking the limit $\lambda\to1$ in Eq. (2.16), we get

$$F(t) = -\frac{1}{12\eta}\frac{1+L_1 t+L_2 t^2}{1+S_1 t+S_2 t^2+S_3 t^3}, \tag{C14}$$

with

$$L_1 = \frac{1+\frac{1}{2}\eta}{1+2\eta}+\frac{6\eta}{1+2\eta}L_2, \tag{C15}$$

$$S_1 = -\frac{3}{2}\frac{\eta}{1+2\eta}+\frac{6\eta}{1+2\eta}L_2, \tag{C16}$$

$$S_2 = -\frac{1}{2}\frac{1-\eta}{1+2\eta}+\frac{1-4\eta}{1+2\eta}L_2, \tag{C17}$$

$$S_3 = -\frac{(1-\eta)^2}{12\eta(1+2\eta)}-\frac{1-\eta}{1+2\eta}L_2. \tag{C18}$$

This coincides with the analytical solution of the PY equation for sticky hard spheres.[7,69,70] From Eq. (A1) we have

$$S(0) = \frac{(1-\eta)^2}{(1+2\eta)^2}[1-\eta+12\eta L_2]^2. \tag{C19}$$

Of course, the results for hard spheres are recovered in the high-temperature limit ($\tau^{-1}\to0$).

[1] M. S. Wertheim, Phys. Rev. Lett. **10**, 321 (1963).
[2] E. Thiele, J. Chem. Phys. **39**, 474 (1963).
[3] S. Asakura and F. Oosawa, J. Chem. Phys. **22**, 1255 (1954).
[4] A. Vrij, Pure Appl. Chem. **48**, 471 (1976).
[5] J. Clément-Cottuz, S. Amokrane, and C. Regnaut, Phys. Rev. E **61**, 1692 (2000).
[6] M. Dijkstra, J. M. Brader, and R. Evans, J. Phys.: Condens. Matter **11**, 10079 (1999).
[7] R. J. Baxter, J. Chem. Phys. **49**, 2770 (1968).
[8] C. Regnaut and J. C. Ravey, J. Chem. Phys. **91**, 1211 (1989).

[9] C. Regnaut and J. C. Ravey, J. Chem. Phys. **92**, 3250 (1990).

[10] C. Robertus, J. G. H. Joosten, and Y. K. Levine, Phys. Rev. A **42**, 4820 (1990).

[11] C. G. de Kruif, P. W. Rouw, W. J. Briels, M. H. G. Duits, A. Vrij, and R. P. May, Langmuir **5**, 422 (1989).

[12] M. H. G. Duits, R. P. May, A. Vrij, and C. G. de Kruif, Langmuir **7**, 62 (1991).

[13] A. Jamnik, D. Bratko, and D. J. Henderson, J. Chem. Phys. **94**, 8210 (1991).

[14] S. V. G. Menon, C. Manohar, and K. S. Rao, J. Chem. Phys. **95**, 9186 (1991).

[15] A. Jamnik, J. Chem. Phys. **102**, 5811 (1995).

[16] C. Regnaut, S. Amokrane, and Y. Heno, J. Chem. Phys. **102**, 6230 (1995).

[17] A. Jamnik, J. Chem. Phys. **105**, 10511 (1995).

[18] S. Amokrane and C. Regnaut, J. Chem. Phys. **106**, 376 (1997).

[19] A. Jamnik, J. Chem. Phys. **109**, 11085 (1998).

[20] J. J. Brey, A. Santos, and F. Castaño, Mol. Phys. **60**, 113 (1987).

[21] G. Stell, J. Stat. Phys. **63**, 1203 (1991).

[22] B. Borštnik, C. G. Jesudason, and G. Stell, J. Chem. Phys. **106**, 9762 (1997).

[23] A. Lang, G. Kahl, C. N. Likos, H. Löwen, and M. Watzlawek, J. Phys.: Condens. Matter **11**, 10143 (1999).

[24] K. Dawson, G. Foffi, M. Fuchs *et al.*, "Higher order glass-transition singularities in colloidal systems with attractive interactions," cond-mat/0008358 (2000).

[25] E. Zaccarelli, G. Foffi, K. A. Dawson, F. Sciortino, and P. Tartaglia, "Mechanical properties of a model of attractive colloidal solutions, cond-mat/0011066 (2000).

[26] M. G. Noro and D. Frenkel, "Extended corresponding-states behavior for particles with variable range attractions," cond-mat/0004033 (2000).

[27] J. A. Barker and D. Henderson, Rev. Mod. Phys. **48**, 587 (1976).

[28] C. Caccamo, Phys. Rep. **274**, 1 (1996).

[29] R. V. Sharma and K. C. Sharma, Physica A **89**, 213 (1977).

[30] W. R. Smith, D. Henderson, and J. A. Barker, J. Chem. Phys. **53**, 508 (1970).

[31] W. R. Smith, D. Henderson, and J. A. Barker, J. Chem. Phys. **55**, 4027 (1971).

[32] D. Henderson, J. A. Barker, and W. R. Smith, J. Chem. Phys. **64**, 4244 (1976).

[33] D. Henderson, O. H. Scalise, and R. Smith, J. Chem. Phys. **72**, 2431 (1980).

[34] J. Chang and S. I. Sandler, Mol. Phys. **81**, 745 (1994).

[35] Y. Tang and B. C.-Y. Lu, J. Chem. Phys. **99**, 9828 (1993).

[36] Y. Tang and B. C.-Y. Lu, J. Chem. Phys. **100**, 3079 (1994).

[37] Y. Tang and B. C.-Y. Lu, J. Chem. Phys. **100**, 6665 (1994).

[38] A. L. Benavides and A. Gil-Villegas, Mol. Phys. **97**, 1225 (1999).

[39] S. B. Yuste and A. Santos, Phys. Rev. A **43**, 5418 (1991).

[40] S. B. Yuste, M. López de Haro, and A. Santos, Phys. Rev. E **53**, 4820 (1996).

[41] D. Henderson, W. G. Madden, and D. D. Fitts, J. Chem. Phys. **64**, 5026 (1976).

[42] I. Nezbeda, Czech. J. Phys., Sect. B **27**, 247 (1977).

[43] C. N. Likos and G. Senatore, J. Phys.: Condens. Matter **7**, 6797 (1995).

[44] S. B. Yuste and A. Santos, J. Chem. Phys. **101**, 2355 (1994).

[45] J. A. Barker and D. Henderson, Can. J. Phys. **44**, 3959 (1967).

[46] Z. W. Salsburg, R. W. Zwanzig, and J. G. Kirkwood, J. Chem. Phys. **21**, 1098 (1953).

[47] J. S. Huang, S. A. Safran, M. W. Kim, and G. S. Grest, Phys. Rev. Lett. **53**, 592 (1984).

[48] L. Vega, E. de Miguel, L. F. Rull, G. Jackson, and I. A. McLure, J. Chem. Phys. **96**, 2296 (1992).

[49] D. A. de Lonngi, P. A. Longgi, and J. Alejandre, Mol. Phys. **71**, 427 (1990).

[50] J. P. Hansen and I. R. McDonald, *Theory of Simple Liquids* (Academic, London, 1986).

[51] L. Acedo, J. Stat. Phys. **99**, 707 (2000).

[52] J. A. Barker and D. Henderson, Mol. Phys. **21**, 1587 (1971).

[53] S. Fishman and M. E. Fisher, Physica A **108**, 1 (1981).

[54] Y. Tago, J. Chem. Phys. **58**, 2096 (1973).

[55] G. A. Vliegenthart and H. N. W. Lekkerkerker, J. Chem. Phys. **112**, 5364 (2000).

[56] J. R. Elliott and L. Hu, J. Chem. Phys. **110**, 3043 (1999).

[57] E. Lomba and N. G. Almarza, J. Chem. Phys. **100**, 8367 (1994).

[58] M. H. J. Hagen and D. Frenkel, J. Chem. Phys. **101**, 4093 (1994).

[59] G. A. Vliegenthart, J. F. M. Lodge, and H. N. W. Lekkerkerker, Physica A **263**, 378 (1999).

[60] E. J. Meijer and F. El Azhar, J. Chem. Phys. **106**, 4678 (1997).

[61] E. J. Meijer and D. Frenkel, J. Chem. Phys. **100**, 6873 (1994).

[62] M. Dijkstra, Phys. Rev. E **58**, 7523 (1998).

[63] M. Dijkstra, R. van Roij, and R. Evans, Phys. Rev. E **59**, 5744 (1999).

[64] A. Santos, S. B. Yuste, and M. López de Haro, J. Chem. Phys. **108**, 3683 (1998).

[65] A. Santos, S. B. Yuste, and M. López de Haro, J. Chem. Phys. **109**, 6814 (1998).

[66] G. Franzese, G. Malescio, A. Skibinsky, S. V. Buldyrev, and H. E. Stanley, "Supercooled fluid-fluid phase transition in three dimensions from a soft-core potential," cond-mat/005184 (2000).

[67] G. Malescio and G. Pellicane, "Simple fluids with complex phase behavior," cond-mat/005214 (2000).

[68] G. Franzese, G. Malescio, A. Skibinsky, S. V. Buldyrev, and H. E. Stanley, Nature (London) **409**, 692 (2001).

[69] S. B. Yuste and A. Santos, J. Stat. Phys. **72**, 703 (1993).

[70] S. B. Yuste and A. Santos, J. Chem. Phys. E **48**, 4599 (1993).